bioRxiv preprint doi: https://doi.org/10.1101/135525; this version posted May 8, 2017. The copyright holder for this preprint (which was not certified by peer review) is the author/funder. All rights reserved. No reuse allowed without permission.

Genome and epigenome engineering CRISPR toolkit for probing *in vivo cis*-regulatory interactions in the chicken embryo

Ruth M Williams[1,*], Upeka Senanayake[1,*], Mara Artibani[1,2], Gunes Taylor[1], Daniel Wells[1], Ahmed Ashour Ahmed[1,2,3] and Tatjana Sauka-Spengler[1,§]

[1] University of Oxford, Weatherall Institute of Molecular Medicine, Radcliffe Department of Medicine, Oxford, OX3 9DS, UK

[2] University of Oxford, Ovarian Cancer Cell Laboratory, Weatherall Institute of Molecular Medicine, Oxford, OX3 9DS, UK

[3] Nuffield Department of Obstetrics and Gynaecology, University of Oxford, Women's Centre, John Radcliffe Hospital, Oxford, OX3 9DU, UK.

* These authors contributed equally

§ Corresponding author: tatjana.sauka-spengler@imm.ox.ac.uk

Keywords: CRISPR, Chicken, enhancer, neural crest, dCas9-LSD1, dCas9-KRAB

Summary Statement: We present an optimised toolkit for efficient genome and epigenome engineering using CRISPR in chicken embryos, with a particular focus on probing gene regulatory interactions during neural crest development.

List of Abbreviations: Genome Engineering (GE), Epigenome Engineering (EGE), single guide RNA (sgRNA), Neural Crest (NC), Transcription Factor (TF), Next Generation Sequencing (NGS), somite stage (ss), Hamburger Hamilton (HH).

bioRxiv preprint doi: https://doi.org/10.1101/135525; this version posted May 8, 2017. The copyright holder for this preprint (which was not certified by peer review) is the author/funder. All rights reserved. No reuse allowed without permission.

Abstract

CRISPR-Cas9 genome engineering has revolutionised all aspects of biological research, with epigenome engineering transforming gene regulation studies. Here, we present a highly efficient toolkit enabling genome and epigenome engineering in the chicken embryo, and demonstrate its utility by probing gene regulatory interactions mediated by neural crest enhancers. First, we optimise efficient guide-RNA expression from novel chick U6-mini-vectors, provide a strategy for rapid somatic gene knockout and establish protocol for evaluation of mutational penetrance by targeted next generation sequencing. We show that CRISPR/Cas9-mediated disruption of transcription factors causes a reduction in their cognate enhancer-driven reporter activity. Next, we assess endogenous enhancer function using both enhancer deletion and nuclease-deficient Cas9 (dCas9) effector fusions to modulate enhancer chromatin landscape, thus providing the first report of epigenome engineering in a developing embryo. Finally, we use the synergistic activation mediator (SAM) system to activate an endogenous target promoter. The novel genome and epigenome engineering toolkit developed here enables manipulation of endogenous gene expression and enhancer activity in chicken embryos, facilitating high-resolution analysis of gene regulatory interactions *in vivo*.

bioRxiv preprint doi: https://doi.org/10.1101/135525; this version posted May 8, 2017. The copyright holder for this preprint (which was not certified by peer review) is the author/funder. All rights reserved. No reuse allowed without permission.

Introduction

Traditionally, *in vivo* loss-of-function studies in the chicken embryo used morpholinos or RNAi approaches. However, short hairpin RNAs have been shown to exert high off-target effects (Mende et al., 2008). While morpholinos have been used successfully to inhibit translation or splicing in a transient fashion, there has been growing concern in the developmental biology field that morpholinos often do not recapitulate mutant phenotypes (Eve et al., 2017; Schulte-Merker and Stainier, 2014) and in some cases may have toxicity issues.

CRISPR-Cas9 genome editing has been successfully used in a number of model organisms including *Drosophila* (Port et al., 2014), mouse (Wang et al., 2013), *Xenopus* (Guo et al., 2014), zebrafish (Hwang et al., 2013), lamprey (Square et al., 2015) and chick (Veron et al., 2015). CRISPR-Cas9 technology requires two components, a single guide RNA (sgRNA) and a Cas9 endonuclease. The sgRNA includes a user defined target-specific 20bp spacer fused directly to a trans-activating RNA (tracrRNA), which is necessary for efficient Cas9 loading. Upon identification of the DNA target site, Cas9 generates a double strand break (DSB). Subsequently, the non-homologous end joining (NHEJ) and more rarely homology directed repair, pathways result in disruption of the targeted genomic region either by introduction of indels or insertion of donor DNA. So far, in the chicken embryo only one CRISPR study has been reported, whereby the authors employed a tetracycline-inducible Cas9 system to knockout a single gene, Pax7, at later stages using Tol2-mediated integration of CRISPR components into somatic cells (Veron et al., 2015). However, this strategy required electroporation of five different plasmids and required longer incubation for genome integration. CRISPR-mediated germ-line editing using cultured primordial germ cells (PGCs) has been employed to develop transgenic chicken lines (Dimitrov et al., 2016; Oishi et al., 2016).

Here we have established a highly efficient *in vivo* genome and epigenome engineering toolkit for studying gene regulatory interactions in the early chicken embryo. Our optimised methods are aimed not only at establishing highly penetrant bi-allelic CRISPR-mediated gene knockouts, but also to enable use of RNA-guided nuclease-deficient dCas9-effector fusion proteins to directly target endogenous enhancers and promoters in order to modulate the chromatin landscape and consequently gene expression in a developing embryo. To this end, we have generated and optimised a novel mini-vector system that uses a chick U6 promoter to mediate high, sustained, efficient sgRNA expression *in vivo*. We have also created a wild-type Cas9 expression vector with a Citrine reporter, as well as several dCas9-effector constructs that enable epigenome manipulation of endogenous enhancers and promoters.

As a proof of principle, we use this novel toolkit to confirm gene regulatory interactions during early neural crest development. The chicken embryo is an ideal model for probing gene regulatory circuits in early development, as it is amenable to *in vivo* perturbation using highly efficient electroporation methods. Moreover, *ex ovo* bilateral electroporation, where each side of the embryo receives a separate set of

bioRxiv preprint doi: https://doi.org/10.1101/135525; this version posted May 8, 2017. The copyright holder for this preprint (which was not certified by peer review) is the author/funder. All rights reserved. No reuse allowed without permission.

plasmids, provides an excellent internal control for each experiment. Our analysis pipeline enabled (i) knockout of upstream transcription factors and assessment of their effects on enhancer activity, (ii) deletion of endogenous enhancers, (iii) epigenetic modulations of endogenous enhancers to assess their role in the expression of the endogenous gene, and (iv) premature activation of endogenous gene loci using an improved targeted gene activation system. The genetic toolkit and optimised protocols developed in this study provide a comprehensive resource to study gene regulatory interactions in the early chicken embryo.

Results and discussion

Optimised mini vectors for sgRNA expression

To achieve efficient genome engineering using the CRISPR/Cas9 system, it is essential to maintain high expression of sgRNAs, which are otherwise rapidly degraded when not incorporated into Cas9 protein (Hendel et al., 2015). Most current RNA Pol III-dependent systems for expression of sgRNAs in amniotes employ human RNU6-1 promoter, a model inherited from siRNA expression vectors (Miyagishi and Taira, 2002). However, the optimised *Drosophila* genome engineering toolkit makes use of an alternative Pol III promoter (U6.3), which exhibits much higher activity in that system (Port et al., 2014).

To build an optimal sgRNA expression system in the chicken embryo, we generated four sgRNA mini expression constructs, each harbouring a different chick U6 promoter (U6.1, U6.2, U6.3 and U6.4) (Kudo and Sutou, 2005), tracrRNA and BsmBI-flanked GoldenGate cloning cassette (Fig. 1A and Fig. S1A). Using a modified GoldenGate assembly approach (supp. protocol 1) we cloned the same spacer targeting the coding region of the FoxD3 gene into each mini-vector. We co-electroporated each U6-mini-vector with a plasmid ubiquitously expressing Cas9 (Cas9-2A-Citrine, Fig. S1B) into the entire epiblast of stage HH4 chicken embryos (Hamburger and Hamilton, 1951) and allowed embryos to develop to stage HH10. To measure the efficiency of sgRNA transcription from different U6 promoters, we analysed editing events caused by Cas9-induced DNA DSBs and subsequent repair by NHEJ at the target site. For this purpose we dissected cranial dorsal neural tubes of four individual embryos for each U6-mini-vector and Cas9-only electroporated controls. We prepared genomic DNA and assessed the presence of DNA hetero-duplexes within the target region using High Resolution Melt Analysis (HRMA, supp. Protocol 2) (Bassett et al., 2013; Dahlem et al., 2012). We observed variable effects from U6.2 and U6.4 promoters, while U6.1 and U6.3 promoters showed more consistent evidence of Cas9-mediated mutations (Fig. 1B), however we found U6.3 yielded the most robust and reproducible effect. Therefore, we used the U6.3 promoter driven sgRNA expression mini-vector in all subsequent experiments.

bioRxiv preprint doi: https://doi.org/10.1101/135525; this version posted May 8, 2017. The copyright holder for this preprint (which was not certified by peer review) is the author/funder. All rights reserved. No reuse allowed without permission.

To further quantify genome editing events produced by U6.3-driven sgRNA we profiled CRISPR-mediated somatic indels using a targeted next generation sequencing approach. Libraries were generated from genomic DNA of six individual embryos (electroporated as described above) by amplifying the sgRNA-targeted region with primers including Illumina sequencing adaptors and custom indexes (adapted from (Gagnon et al., 2014). After mapping the reads to the FoxD3 amplicon, we used the CRISPResso tool (Pinello et al., 2016) to determine the indel frequency and observed that all the experimental embryos had a higher percentage of NHEJ events than the controls (where the modified reads are a consequence of five recurrent SNPs). The percentage of modified reads for two representative embryos as well as the alignment of a subset of deletions identified in the experimental embryos are shown (Fig. 1C).

Targeting transcription factors associated with enhancers

Having established an efficient sgRNA delivery protocol, we next used CRISPR/Cas9-mediated gene knockout to probe input-enhancer interactions, focusing on targeting transcription factors implicated in neural crest development. To this end, we designed sgRNAs to target Msx1, Pax7, Sox9, c-Myb and Ets1, previously demonstrated to act as upstream regulatory inputs into either the FoxD3 enhancer NC1 (Simoes-Costa et al., 2012) or the Sox10 enhancer 10E2 (Betancur et al., 2010) (Fig. 2A). We designed sgRNAs targeting the essential DNA binding domains encoded within each of these genes (Fig. 2B) to ensure loss of transcription factor function. sgRNAs were predicted manually by scanning regions of interest for proximal PAM sequences, while final choices were selected based on low self-complementarity and unique alignment to the chick genome. sgRNA spacers were then cloned into the U6.3 mini-vector and tested individually as above (Fig. 2C). In addition to HRMA, we have also adopted an alternative T7 endonuclease assay (Supp. Protocol 3) to validate candidate sgRNAs. The selected sgRNAs were co-electroporated with ubiquitous Cas9-2A-Citrine and either FoxD3 (NC1) or Sox10 (10E2) enhancer driving mCherry, to assess enhancer reporter activity in the condition of upstream transcription factor knockout. We performed bilateral electroporations at HH4, with the left side receiving the target sgRNA+Cas9 and the right side receiving a scrambled control sgRNA+Cas9 (Fig. 2D) as an internal control. Both sides received the mCherry reporter containing the tested enhancer. Consistent with previous morpholino-based studies (Betancur et al., 2010; Simoes-Costa et al., 2012), we found that knockout of either Msx1, Pax7 or Ets1 strongly reduces mCherry expression mediated by the NC1 enhancer at 5-7 somite stage (ss) in 70%, 100% and 71.4% of cases, respectively (Figs. 2E-G, 2E'-G'; n=10, 7 and 11 respectively). At later stages however, only Pax7 knockouts had a moderate effect (33.3%). Similarly, knockout of Sox9, c-Myb and Ets1 led to a decrease in the activity of Sox10 enhancer, 10E2, with a 100% penetrance for all factors at 5-7ss (Figs. 2H-J, 2H'-J'). However, we observed a decreased effect at later stages (8-10ss; Sox9 14.3% and Ets1 50%), in line with previous findings that Sox10 auto-regulates to maintain Sox10E2 activity and Sox10 expression (Betancur et al., 2010; Wahlbuhl et al., 2012). These results demonstrate that the CRISPR/Cas9 system is highly efficient in the chicken embryo and provides an excellent alternative to previously used

bioRxiv preprint doi: https://doi.org/10.1101/135525; this version posted May 8, 2017. The copyright holder for this preprint (which was not certified by peer review) is the author/funder. All rights reserved. No reuse allowed without permission.

technologies such as morpholinos, while enabling an independent confirmation of data from previous neural crest *cis*-regulatory analyses (Betancur et al., 2010; Simoes-Costa et al., 2012).

Targeting enhancers for DSB-NHEJ mediated removal

To fully characterise enhancer function, it is important to study them in their endogenous cellular context. Thus we used our newly developed CRISPR/Cas9 tools to remove the endogenous FoxD3-NC1 cranial enhancer (Fig 3A) *in vivo* and assess the consequence of its deletion on the expression of FoxD3. We designed and tested sgRNAs flanking the core NC1 enhancer region and used these in conjunction with Cas9-2A-Citrine to remove the enhancer. We assayed the effect of NC1 enhancer knockout in individual embryos, using bilateral electroporation where target sgRNAs+Cas9 were introduced on the left and scrambled control sgRNA+Cas9 on the right side of the same embryo (Fig 3C). Embryos were reared to the desired stages, dorsal neural tubes from experimental (left) and control (right) sides were dissected, and the effect on expression of endogenous FoxD3 was assessed using quantitative RT PCR (qPCR). Using the absolute quantification method with the same standard curve cDNA across all experiments, allowed us to define the level of FoxD3 at the onset of its expression on the control side as a threshold (~0.35 arbitrary units). We observed a decrease in FoxD3 expression on the experimental side in 66.7% of embryos analysed at 5-8ss (n=9) (Fig. 3D). This demonstrates that NC1 endogenous enhancer activity is essential for the onset of the FoxD3 expression.

Targeting enhancers for epigenome modification

To further refine our analysis of enhancer function *in vivo*, we adopted targeted epigenome engineering (EGE) approaches to alter the chromatin landscape associated with active enhancers. Hitherto, such techniques have only been used *in vitro* (Kearns et al., 2015; Mendenhall et al., 2013; Thakore et al., 2015). To bring EGE methodology into the developing chicken embryo we generated chick expression constructs driving fusion proteins of the catalytically inactive *S. pyogenes* Cas9 (dCas9) with lysine specific demethylase 1 (LSD1) or the Krüppel-associated box (KRAB) domain (Fig. S1C). LSD1 is a lysine-specific demethylase that catalyses the removal of H3K4me1/2 and H3K9me2, which are associated with active and repressive chromatin respectively (Shi et al., 2004) (Fig 3E), whereas the KRAB domain is thought to recruit a chromatin compaction complex thus rendering enhancers inaccessible (Sripathy et al., 2006) (Fig 3G). LSD1 was first used as an effector that demethylates enhancer-associated histone methylation with TALEN technology leading to inactivation of targeted enhancers (Mendenhall et al., 2013). More recently, *N.meningitidis* dCas9 fusions with either LSD1 or KRAB were used to inactivate known Oct4 *cis*-regulatory elements in mouse embryonic stem cells (Kearns et al., 2015) and human codon-optimised *S. pyogenes* dCas9-KRAB was used to inactivate HS2 enhancer within the globin locus control region in K562 erythroid leukaemia cells (Thakore et al., 2015).

bioRxiv preprint doi: https://doi.org/10.1101/135525; this version posted May 8, 2017. The copyright holder for this preprint (which was not certified by peer review) is the author/funder. All rights reserved. No reuse allowed without permission.

In order to efficiently repress enhancer activity in chicken embryos, we used five sgRNAs tiled across each target enhancer. sgRNA spacers were cloned into the U6.3 expression mini-vector and tested individually, as described above. Pools of five selected sgRNAs per enhancer were co-electroporated bilaterally with the ubiquitous dCas9-effector fusion construct on the left side of the embryo. The right, control side was electroporated with equal molar quantity of scrambled control sgRNA mini-vector combined with the same dCas9-effector (Fig. 3C). Embryos were allowed to develop to the desired stages and then the experimental and control cranial regions were dissected. The effect of chromatin EGE modification at the targeted enhancer was assessed by measuring the levels of endogenous target gene using quantitative RT-PCR (qPCR), as described above. The time point for qPCR analysis of each tested enhancer was set to approximately three hours before the fluorescent reporter can first be detected, to account for the maturation time of the fluorophore. The dCas9-LSD1 targeted demethylation approach was first applied to repress the activity of the Sox10 enhancer 10E2 (Betancur et al., 2010). Since no changes were observed in the endogenous level of Sox10 on the experimental versus control side at any of the stages tested (4-8ss) (Fig. S2A), we reasoned that 10E2 element might not be the earliest enhancer controlling Sox10 expression. This assumption is supported by the observation that its fluorescent reporter activity only starts to be detected at 7-9 ss. Using epigenomic profiling we have identified a novel Sox10 enhancer (enhancer 99, Fig. 3B), yielding Sox10-like fluorescent reporter activity from 4ss. We hypothesised that this element may be important for the onset of endogenous Sox10 expression. Indeed when dCas9-LSD1 activity was targeted to the enh-99, we achieved a reproducible (100%, n=9, $**p<0.01$) knockdown of endogenous Sox10 expression on the experimental versus control side, in embryos ranging from 5-7ss (Fig. 3F). We next targeted dCas9-KRAB to the FoxD3 enhancer NC1, whose fluorescent reporter activity is first detectable at 5ss. When analysed at 4-6ss, we observed a decrease in endogenous FoxD3 expression on the experimental side in 57% of embryos (n=14) (Fig. 3H), suggesting that while NC1 is required for proper FoxD3 expression different, potentially earlier acting enhancer(s) may co-regulate FoxD3 onset. Interestingly, targeting dCas9-LSD1 to NC1 enhancer had a milder effect on FoxD3 gene expression (Fig. S2C), where 44.4% embryos (n=9) showed a down-regulation of FoxD3. We also observed down-regulation of Sox10 in 62.5% of embryos (n=11) when we targeted dCas9-KRAB to Sox10 enh-99 (Fig S2D). However, 10E2 targeted dCas9-KRAB had a milder effect on Sox10 expression, showing an effect in 33.3% (n=15) of embryos assayed (Fig S2B). Overall this suggests that the two approaches have different mechanistic modes of action (Kearns et al., 2015), with one being efficient only at stopping the initiation of the enhancer activity (dCas9-LSD1) and the other (dCas9-KRAB) allowing active repression even of elements that are already actively engaged in enhancing gene expression. Applying two different approaches we show that we can successfully decommission NC specific enhancers *in vivo*, as assessed by reduced expression of the genes they control. This demonstrates both the link between a putative enhancer and target as well as its importance to downstream gene activity. The constructs generated and

bioRxiv preprint doi: https://doi.org/10.1101/135525; this version posted May 8, 2017. The copyright holder for this preprint (which was not certified by peer review) is the author/funder. All rights reserved. No reuse allowed without permission.

optimised here provide a novel toolkit, which can be readily applied to study *in vivo* enhancer function, in an efficient, affordable manner.

Premature activation of endogenous gene expression *in vivo* using CRISPR-ON

To complement our loss of function (gene and enhancer) studies, we have also adapted the dCas9-VP64-mediated activation of endogenous gene transcription *in vivo*. VP64 is a well-established transcriptional activator domain that consists of a tetrameric repeat of the minimal activation domain of the herpes simplex protein VP16 (Seipel et al., 1992) and dCas9-VP64 fusion has been successfully used in CRISPR-ON experiments to ectopically activate gene expression (Cheng et al., 2013; Guo et al., 2017). Here, we use a dCas9-VP64 fusion in conjunction with the synergistic activation mediator (SAM) system (Konermann et al., 2015). SAM is a three-component system. The first is a modified U6 vector driving expression of a sgRNA containing a modified tracrRNA scaffold (Fig. S1A), which provides binding sites for cognate bacteriophage coat protein MS2. The second component is MS2-effector expression vector, in which the cognate protein (MS2) is fused to an effector domain, in this case VP64. As the third component, dCas9-VP64 expression plasmid was used (Fig. S1D). Co-expression of all three components results in saturation of the targeted site with effector molecules, thus enabling a 'CRISPR-ON' response using just one sgRNA (Fig. 4A). We tested five sgRNAs to the Sox10 promoter and used the most efficient one to prematurely activate Sox10 expression using the dCas9-VP64/SAM system. Following bilateral electroporation at HH4, we observed an increase in Sox10 expression at 3-4ss on experimental versus control side of the embryo, indicating premature activation of the gene (50% embryos, n=12, Fig. 4B).

Here, we have optimised CRISPR-Cas9 approaches to perform both genome and epigenome engineering in the early chicken embryo and probe gene regulatory interactions. Our genome editing-mediated transcription factor knockouts in the neural crest gene regulatory network confirms linkages suggested by transient morpholino approaches, but does so in a much more efficient, penetrant, and cost-effective manner. Moreover, our novel methodology enables both deletion and activation of enhancers and promoters. Previously, altering gene regulatory interactions with epigenome engineering approaches for targeted modulation of chromatin features associated with active enhancers and promoters has only been attempted *in vitro* (Kearns et al., 2015; Konermann et al., 2015; Mendenhall et al., 2013; Thakore et al., 2015). The novel toolkit presented here extends the possibility of epigenome engineering to an *in vivo* system. Although we focus on the early chicken embryo due to its accessibility for experimental manipulation via electroporation, we propose that such approaches could be easily adapted to other amniotes.

bioRxiv preprint doi: https://doi.org/10.1101/135525; this version posted May 8, 2017. The copyright holder for this preprint (which was not certified by peer review) is the author/funder. All rights reserved. No reuse allowed without permission.

Figure legends

Figure 1. Optimising sgRNA mini-vectors. (A) Schematic representation of U6 sgRNA expression mini-vector. The 3.5kb plasmid contains a U6 promoter, BsmBI-flanked sgRNA cassette, followed by the tracrRNA scaffold and U6 terminator. (B) Efficacy of four U6 promoters was tested using High Resolution Melt Analysis (HRMA). Each HRMA plot shows normalised melt curves from embryos co-electroporated with Cas9 and one of the U6 mini-vectors (U6.1, U6.2, U6.3 and U6.4) containing the same sgRNA targeted to the FoxD3 gene and control Cas9-only electroporated embryos. Each HRMA curve is the melting profile of re-annealed amplicons generated from a single embryo, showing temperature shift when compared to Cas9-only controls (red). Relative Fluorescence Units (RFU) for experimental samples were normalised to the control samples in each case. (C) NGS validation of genome editing events produced by U6.3-driven FoxD3 sgRNA with ubiquitous Cas9. The chick FoxD3 genomic structure is shown together with a schematic representation of the NGS library preparation protocol. Pie charts show the percentage of unmodified and NHEJ reads for two representative embryos (control and experimental). Alignment shows of a subset of 28 deletion variants identified in the experimental embryos.

Figure 2. Targeting enhancer inputs reduces enhancer activity. (A) Schematic representation of the TF inputs into 10E2 and NC1 enhancers. (A') mCherry reporter activity in the cranial neural crest controlled by 10E2 and NC1 enhancers. (B) Approximate positions of sgRNAs targeting five TFs are shown on the schematics of respective gene loci. (C) HRMA plots show temperature-shifted difference curves for each sgRNA used. Experimental samples normalised to the control samples (Cas9 only, red lines) show significant deviation in each case. (D) Schematic of bilateral electroporation. Target sgRNA, Cas9-2A-Citrine and enhancer-mCherry are co-electroporated on the left (magenta) and scrambled control sgRNAs with the same Cas9 and reporter on the right side of the embryo (blue). (E,F,G) GE-mediated disruption of Msx1, Pax7 or Ets1 result in a decrease in NC1 driven mCherry on the experimental, left side of the embryo (E',F',G') same embryos as in (E,F,G) showing Cas9-2A-Citrine signal and brightfield view of the electroporated embryo. (H,I,J) GE-mediated disruption of Sox9, cMyb or Ets1 results in a decrease in 10E2 driven mCherry on the experimental side. (H',I',J') same embryos as in (H,I,J) showing Cas9-2A-Citrine signal and brightfield view of the electroporated embryo. All experiments were performed in triplicates; representative embryos are shown.

Figure 3. Epigenome engineering to directly manipulate endogenous enhancer activity. (A) FoxD3 enhancer, NC1 driven Citrine expression at 6ss. (B) Novel Sox10 enhancer, (enh-99), controls Sox10-like Citrine expression in cranial neural crest at 7ss. (C) Schematic of bilateral electroporation. (D) Deletion of the NC1 enhancer using Cas9 and sgRNAs flanking the enhancer core region causes a down-regulation of FoxD3 expression on the experimental side (left, magenta) versus control (right, blue) side which received scrambled control sgRNA, (77.7% of embryos, n=16). (E and G) Schematics depict epigenetic enhancer

bioRxiv preprint doi: https://doi.org/10.1101/135525; this version posted May 8, 2017. The copyright holder for this preprint (which was not certified by peer review) is the author/funder. All rights reserved. No reuse allowed without permission.

silencing mechanisms by dCas9-LSD1 (E) and dCas9-KRAB (G) fusion proteins. (F) 5 guides targeted to the Sox10 enh-99, co-electroporated with dCas9-LSD1 cause a down-regulation of endogenous Sox10 expression at 5-7ss on the experimental side compared to the control side. The effect was observed in 100% of embryos assayed (n=9, $**p<0.001$ using chi-squared statistical test). (H) 5 guides targeted to NC1 enhancer, co-electroporated with dCas9-KRAB cause a down-regulation of endogenous FoxD3 expression on the experimental versus control side, (57% of embryos, n=14). All experiments were performed in triplicate, representative embryos are shown, error bars represent the standard deviation.

Figure 4. CRISPR-ON mediated activation of endogenous Sox10 promoter using Synergistic Activation Mediator (SAM) method. (A) Schematic representation of VP64-dCas9-MS2 SAM complex. (B) One sgRNA targeting the Sox10 promoter co-electroporated with dCas9-VP64 and VP64-MS2 fusion constructs causes a premature activation of Sox10 transcription on the experimental (magenta, left) as compared to the control side (blue, right). (50% embryos, n=12, $*p<0.05$). All experiments were performed in triplicate, representative embryos are shown, error bars represent the standard deviation.

Materials and Methods

Construct cloning

Chick U6 sgRNA expression mini-vectors were cloned by replacing the BsaI-flanked cassette from pNG1-pNG4 vector backbones (Cermak et al., 2011) (Addgene #30985-8) with custom-synthesised gBlocks (IDT) containing chick cU6_1-4 promoters (Kudo and Sutou, 2005).

pCAGGs_Cas9-2A-Citrine construct was generated by removing IRES-H2B-RFP cassette from pCI_H2B-RFP vector (Betancur et al., 2010) and inserting Cas9-2A-Citrine fragment by In-fusion HD (Clontech, cat #638910) cloning.

To construct the pX330 dCas9-LSD1 vector, Cas9m4-VP64 was amplified from (Addgene #47319) and cloned into pX330 (Addgene #42230). VP64 was then removed by EcoRI digest and LSD1 was inserted from EMM67 (Addgene #49043) (Mendenhall et al., 2013). pX330 dCas9-KRAB was generated by In-fusion of a synthetic gBlock containing the KRAB sequence into the EcoRI linearised pX330-dCas9-LSD vector.

pCAGGs-dCas9-KRAB-T2A-GFP was generated by amplifying dCas9-KRAB-T2A-GFP sequence from pLV hUbC dCas9 KRAB T2A GFP (Addgene #71237) and cloning into the pCI-H2B-RFP vector linearised by NotI and XhoI.

bioRxiv preprint doi: https://doi.org/10.1101/135525; this version posted May 8, 2017. The copyright holder for this preprint (which was not certified by peer review) is the author/funder. All rights reserved. No reuse allowed without permission.

The MS2-VP64 construct was generated by removing the IRES-H2B-RFP cassette from pCI_H2B-RFP vector (Betancur et al., 2010) and by inserting the MS2 and VP64 fragments (amplified from Addgene #61423 and #47319, respectively) using 2-fragment Infusion cloning.

Embryo culture and electroporations

Fertilised wild type chicken eggs were obtained from Henry Stewart & Co (Norfolk). Staged according to (Hamburger and Hamilton, 1951) and electroporated as previously described (Sauka-Spengler and Barembaum, 2008; Simoes-Costa et al., 2012). Electroporation conditions are detailed in a separate protocol (Supplemental Info).

GE reagent cloning and validation

Detailed standardised protocols describing guide RNA selection, GoldenGate cloning, bilateral electroporation and validation by HRMA, T7 assays and NGS are available as Supplemental Info and at our resource page (http://www.tsslab.co.uk/resources). All plasmids are available from Addgene (https://www.addgene.org/Tatjana_Sauka-Spengler/).

qPCR analysis of endogenous levels

RNA extractions of dissected embryonic tissue were carried out using the RNAqueous®-Micro Kit (Life Technologies, cat # AM1931). Oligo-dT-primed cDNA was synthesised using Superscript III reverse transcriptase (Invitrogen) and qPCRs performed using Fast SYBR Green reagent (ThermoFisher, cat #4385612) on the Applied Biosystems 7500 Fast Real-Time PCR System. Standard curve method was used to quantify the gene expression. In all embryos, contralateral side was used as an internal control. Statistical significance of bilateral electroporations was determined by generating a control embryo group that received scrambled sgRNAs on both sides and calculating p-values using chi-squared statistical test, based on contingency tables comparing control and experimental embryo groups. *$p<0.05$, **$p<0.01$.

Imaging analysis

Embryos were imaged on an Olympus MVX10 stereomicroscope with 2-2.5x objective using Axio Vision 4.8 software.

Acknowledgements

We thank Prof Tudor Fulga for helpful advice on the project and the manuscript and Francesco Camera for technical assistance.

bioRxiv preprint doi: https://doi.org/10.1101/135525; this version posted May 8, 2017. The copyright holder for this preprint (which was not certified by peer review) is the author/funder. All rights reserved. No reuse allowed without permission.

Competing interests

The authors declare no competing or financial interests.

Author contributions

US, RW and TSS conceived the study. US generated the constructs and RW performed majority of the GE and EGE experiments. MA generated dCas9-VP64/SAM constructs and established protocols for targeted NGS validation of GE events. GT optimised sgRNA GoldenGate cloning and built dCas9-KRAB constructs. DW helped build and test U6 mini-vectors and developed methods for multiple sgRNA expression; RW, MA and TSS analysed the data; RW and TSS wrote the manuscript; RW, US, MA, GT, AA, TSS edited the manuscript; TSS supervised the study.

Funding

This study was funded by MRC (G0902418), OCA (MA), Lister Institute summer studentship to DW.

bioRxiv preprint doi: https://doi.org/10.1101/135525; this version posted May 8, 2017. The copyright holder for this preprint (which was not certified by peer review) is the author/funder. All rights reserved. No reuse allowed without permission.

References

Bassett, A.R., C. Tibbit, C.P. Ponting, and J.L. Liu. 2013. Highly efficient targeted mutagenesis of Drosophila with the CRISPR/Cas9 system. *Cell Rep*. 4:220-228.

Betancur, P., M. Bronner-Fraser, and T. Sauka-Spengler. 2010. Genomic code for Sox10 activation reveals a key regulatory enhancer for cranial neural crest. *Proc Natl Acad Sci U S A*. 107:3570-3575.

Cermak, T., E.L. Doyle, M. Christian, L. Wang, Y. Zhang, C. Schmidt, J.A. Baller, N.V. Somia, A.J. Bogdanove, and D.F. Voytas. 2011. Efficient design and assembly of custom TALEN and other TAL effector-based constructs for DNA targeting. *Nucleic Acids Res*. 39:e82.

Cheng, A.W., H. Wang, H. Yang, L. Shi, Y. Katz, T.W. Theunissen, S. Rangarajan, C.S. Shivalila, D.B. Dadon, and R. Jaenisch. 2013. Multiplexed activation of endogenous genes by CRISPR-on, an RNA-guided transcriptional activator system. *Cell Res*. 23:1163-1171.

Dahlem, T.J., K. Hoshijima, M.J. Jurynec, D. Gunther, C.G. Starker, A.S. Locke, A.M. Weis, D.F. Voytas, and D.J. Grunwald. 2012. Simple methods for generating and detecting locus-specific mutations induced with TALENs in the zebrafish genome. *PLoS Genet*. 8:e1002861.

Dimitrov, L., D. Pedersen, K.H. Ching, H. Yi, E.J. Collarini, S. Izquierdo, M.C. van de Lavoir, and P.A. Leighton. 2016. Germline Gene Editing in Chickens by Efficient CRISPR-Mediated Homologous Recombination in Primordial Germ Cells. *PLoS One*. 11:e0154303.

Eve, A.M., E.S. Place, and J.C. Smith. 2017. Comparison of Zebrafish tmem88a mutant and morpholino knockdown phenotypes. *PLoS One*. 12:e0172227.

Gagnon, J.A., E. Valen, S.B. Thyme, P. Huang, L. Akhmetova, A. Pauli, T.G. Montague, S. Zimmerman, C. Richter, and A.F. Schier. 2014. Efficient mutagenesis by Cas9 protein-mediated oligonucleotide insertion and large-scale assessment of single-guide RNAs. *PLoS One*. 9:e98186.

Guo, J., D. Ma, R. Huang, J. Ming, M. Ye, K. Kee, Z. Xie, and J. Na. 2017. An inducible CRISPR-ON system for controllable gene activation in human pluripotent stem cells. *Protein Cell*.

Guo, X., T. Zhang, Z. Hu, Y. Zhang, Z. Shi, Q. Wang, Y. Cui, F. Wang, H. Zhao, and Y. Chen. 2014. Efficient RNA/Cas9-mediated genome editing in Xenopus tropicalis. *Development*. 141:707-714.

Hamburger, V., and H.L. Hamilton. 1951. A series of normal stages in the development of the chick embryo. *J Morphol*. 88:49-92.

Hendel, A., R.O. Bak, J.T. Clark, A.B. Kennedy, D.E. Ryan, S. Roy, I. Steinfeld, B.D. Lunstad, R.J. Kaiser, A.B. Wilkens, R. Bacchetta, A. Tsalenko, D. Dellinger, L. Bruhn, and M.H. Porteus. 2015. Chemically modified guide RNAs enhance CRISPR-Cas genome editing in human primary cells. *Nat Biotechnol*. 33:985-989.

Hwang, W.Y., Y. Fu, D. Reyon, M.L. Maeder, S.Q. Tsai, J.D. Sander, R.T. Peterson, J.R. Yeh, and J.K. Joung. 2013. Efficient genome editing in zebrafish using a CRISPR-Cas system. *Nat Biotechnol*. 31:227-229.

Kearns, N.A., H. Pham, B. Tabak, R.M. Genga, N.J. Silverstein, M. Garber, and R. Maehr. 2015. Functional annotation of native enhancers with a Cas9-histone demethylase fusion. *Nat Methods*. 12:401-403.

Konermann, S., M.D. Brigham, A.E. Trevino, J. Joung, O.O. Abudayyeh, C. Barcena, P.D. Hsu, N. Habib, J.S. Gootenberg, H. Nishimasu, O. Nureki, and F. Zhang. 2015. Genome-scale transcriptional activation by an engineered CRISPR-Cas9 complex. *Nature*. 517:583-588.

Kudo, T., and S. Sutou. 2005. Usage of putative chicken U6 promoters for vector-based RNA interference. *J Reprod Dev*. 51:411-417.

Mende, M., N.A. Christophorou, and A. Streit. 2008. Specific and effective gene knock-down in early chick embryos using morpholinos but not pRFPRNAi vectors. *Mech Dev*. 125:947-962.

bioRxiv preprint doi: https://doi.org/10.1101/135525; this version posted May 8, 2017. The copyright holder for this preprint (which was not certified by peer review) is the author/funder. All rights reserved. No reuse allowed without permission.

Mendenhall, E.M., K.E. Williamson, D. Reyon, J.Y. Zou, O. Ram, J.K. Joung, and B.E. Bernstein. 2013. Locus-specific editing of histone modifications at endogenous enhancers. *Nat Biotechnol*. 31:1133-1136.

Miyagishi, M., and K. Taira. 2002. U6 promoter-driven siRNAs with four uridine 3' overhangs efficiently suppress targeted gene expression in mammalian cells. *Nat Biotechnol*. 20:497-500.

Oishi, I., K. Yoshii, D. Miyahara, H. Kagami, and T. Tagami. 2016. Targeted mutagenesis in chicken using CRISPR/Cas9 system. *Sci Rep*. 6:23980.

Pinello, L., M.C. Canver, M.D. Hoban, S.H. Orkin, D.B. Kohn, D.E. Bauer, and G.C. Yuan. 2016. Analyzing CRISPR genome-editing experiments with CRISPResso. *Nat Biotechnol*. 34:695-697.

Port, F., H.M. Chen, T. Lee, and S.L. Bullock. 2014. Optimized CRISPR/Cas tools for efficient germline and somatic genome engineering in Drosophila. *Proc Natl Acad Sci U S A*. 111:E2967-2976.

Sauka-Spengler, T., and M. Barembaum. 2008. Gain- and loss-of-function approaches in the chick embryo. *Methods Cell Biol*. 87:237-256.

Schulte-Merker, S., and D.Y. Stainier. 2014. Out with the old, in with the new: reassessing morpholino knockdowns in light of genome editing technology. *Development*. 141:3103-3104.

Seipel, K., O. Georgiev, and W. Schaffner. 1992. Different activation domains stimulate transcription from remote ('enhancer') and proximal ('promoter') positions. *EMBO J*. 11:4961-4968.

Shi, Y., F. Lan, C. Matson, P. Mulligan, J.R. Whetstine, P.A. Cole, R.A. Casero, and Y. Shi. 2004. Histone demethylation mediated by the nuclear amine oxidase homolog LSD1. *Cell*. 119:941-953.

Simoes-Costa, M.S., S.J. McKeown, J. Tan-Cabugao, T. Sauka-Spengler, and M.E. Bronner. 2012. Dynamic and Differential Regulation of Stem Cell Factor FoxD3 in the Neural Crest Is Encrypted in the Genome. *PLoS genetics*. 8:e1003142.

Square, T., M. Romasek, D. Jandzik, M.V. Cattell, M. Klymkowsky, and D.M. Medeiros. 2015. CRISPR/Cas9-mediated mutagenesis in the sea lamprey Petromyzon marinus: a powerful tool for understanding ancestral gene functions in vertebrates. *Development*. 142:4180-4187.

Sripathy, S.P., J. Stevens, and D.C. Schultz. 2006. The KAP1 corepressor functions to coordinate the assembly of de novo HP1-demarcated microenvironments of heterochromatin required for KRAB zinc finger protein-mediated transcriptional repression. *Mol Cell Biol*. 26:8623-8638.

Thakore, P.I., A.M. D'Ippolito, L. Song, A. Safi, N.K. Shivakumar, A.M. Kabadi, T.E. Reddy, G.E. Crawford, and C.A. Gersbach. 2015. Highly specific epigenome editing by CRISPR-Cas9 repressors for silencing of distal regulatory elements. *Nat Methods*. 12:1143-1149.

Veron, N., Z. Qu, P.A. Kipen, C.E. Hirst, and C. Marcelle. 2015. CRISPR mediated somatic cell genome engineering in the chicken. *Dev Biol*. 407:68-74.

Wahlbuhl, M., S. Reiprich, M.R. Vogl, M.R. Bosl, and M. Wegner. 2012. Transcription factor Sox10 orchestrates activity of a neural crest-specific enhancer in the vicinity of its gene. Nucleic *Acids Res*. 40:88-101.

Wang, H., H. Yang, C.S. Shivalila, M.M. Dawlaty, A.W. Cheng, F. Zhang, and R. Jaenisch. 2013. One-step generation of mice carrying mutations in multiple genes by CRISPR/Cas-mediated genome engineering. *Cell*. 153:910-918.

Williams et al. Figure 1

bioRxiv preprint doi: https://doi.org/10.1101/135525; this version posted May 8, 2017. The copyright holder for this preprint (which was not certified by peer review) is the author/funder. All rights reserved. No reuse allowed without permission.

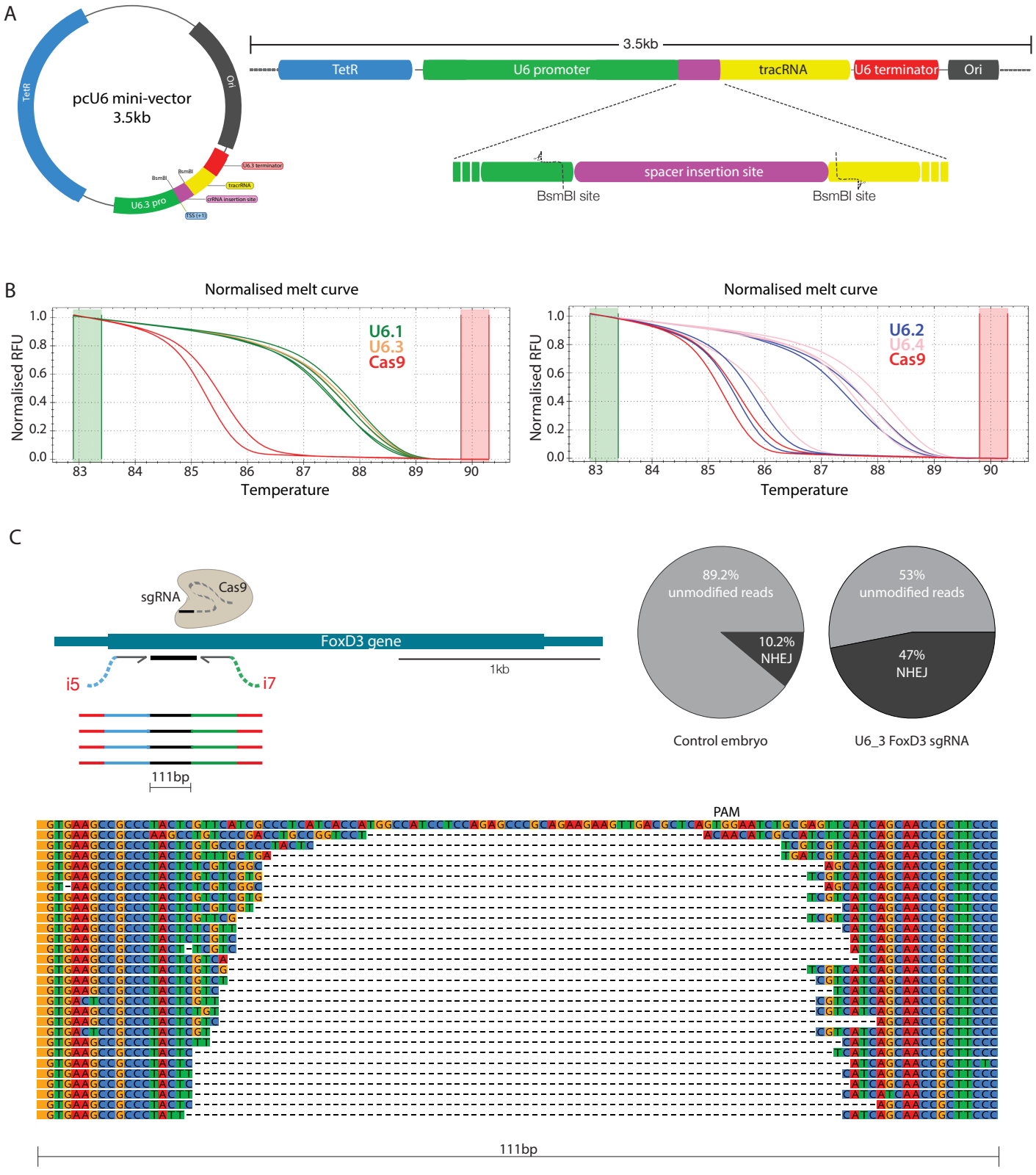

bioRxiv preprint doi: https://doi.org/10.1101/135525; this version posted May 8, 2017. The copyright holder for this preprint (which was not certified by peer review) is the author/funder. All rights reserved. No reuse allowed without permission.

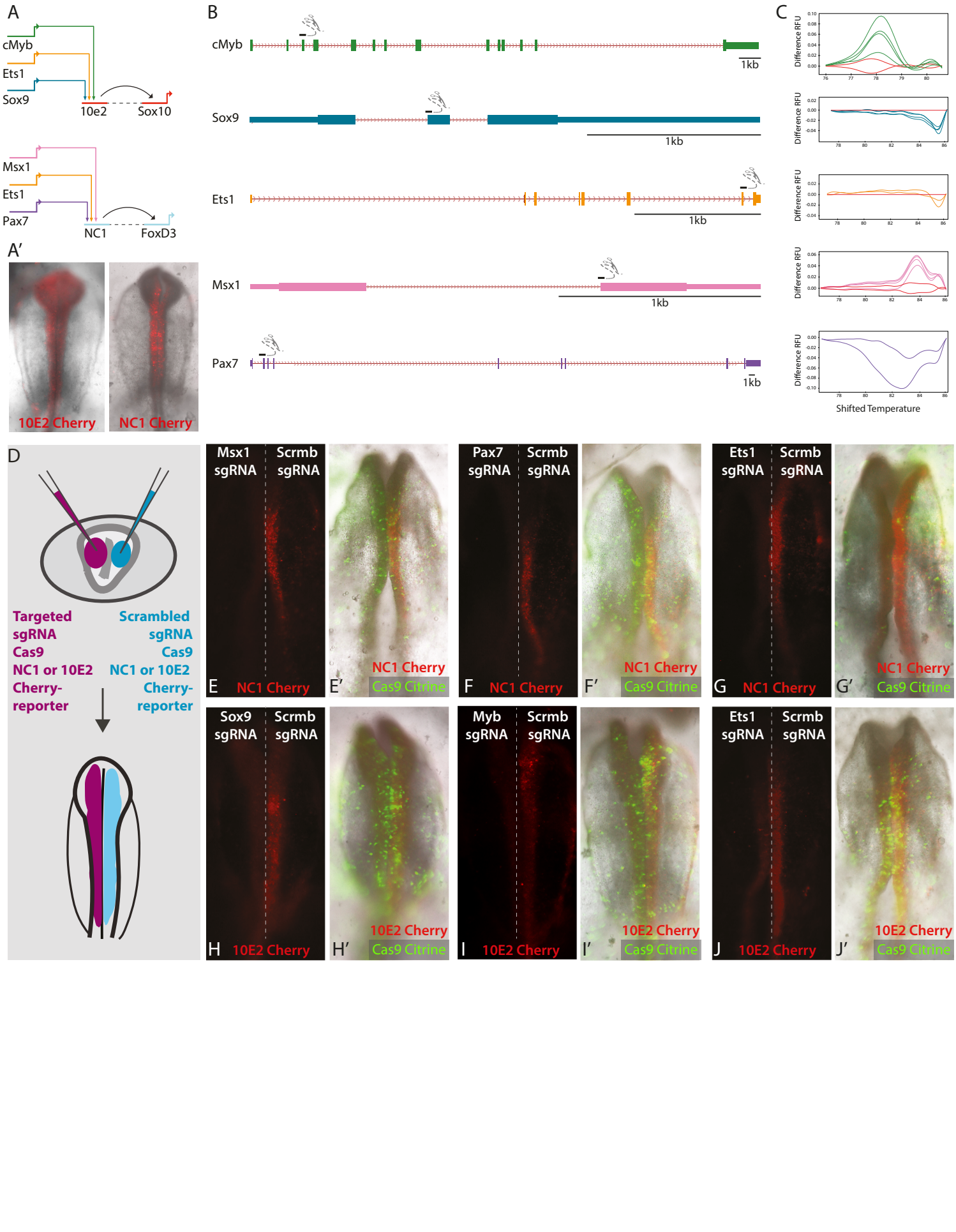

bioRxiv preprint doi: https://doi.org/10.1101/135525; this version posted May 8, 2017. The copyright holder for this preprint (which was not certified by peer review) is the author/funder. All rights reserved. No reuse allowed without permission.

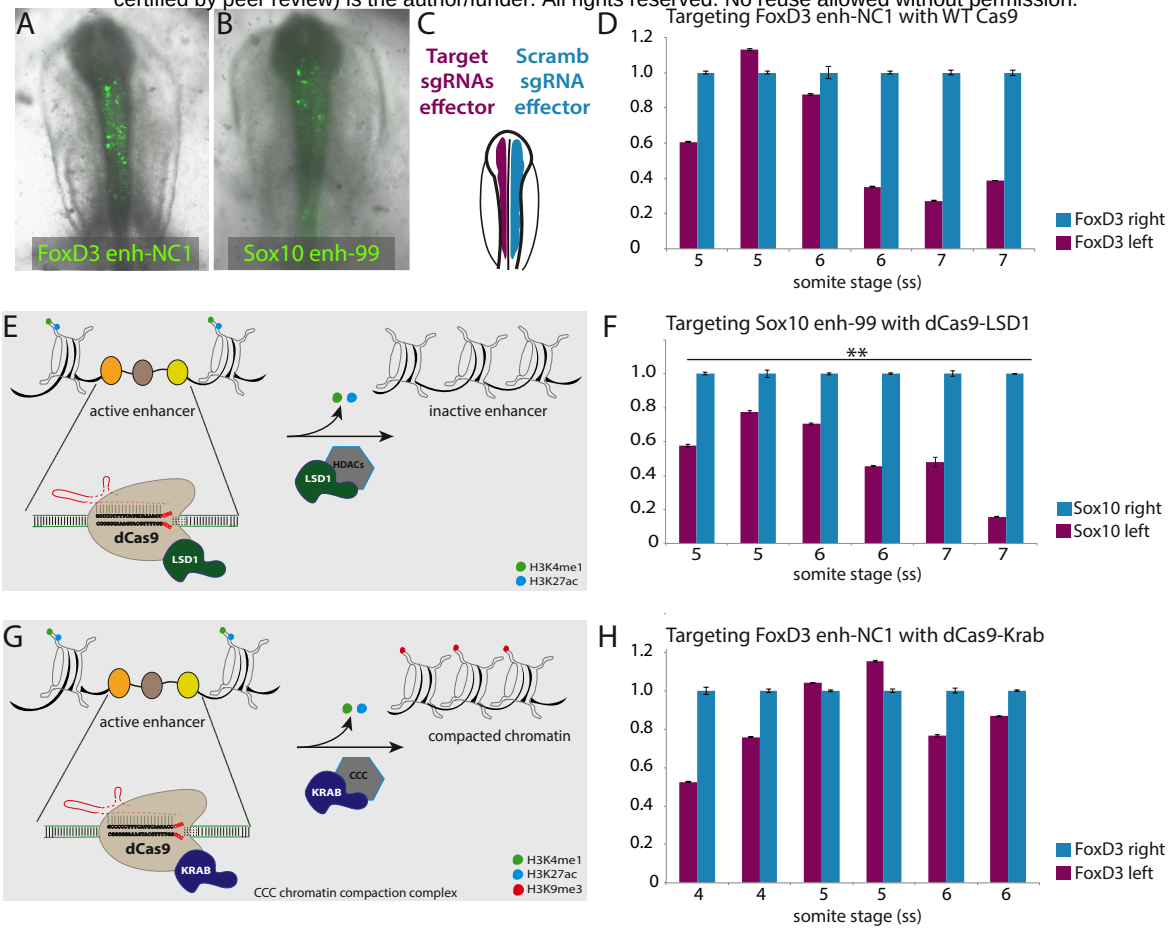

Williams et al. Figure 4
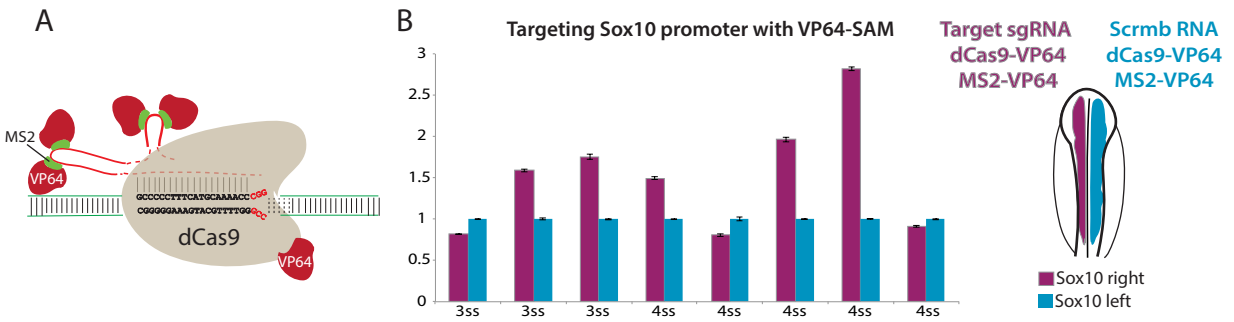
bioRxiv preprint doi: https://doi.org/10.1101/135525; this version posted May 8, 2017. The copyright holder for this preprint (which was not certified by peer review) is the author/funder. All rights reserved. No reuse allowed without permission.